Plant Molecular Biology (2022) 109:505–522
https://doi.org/10.1007/s11103-021-01191-3

Acylsugars protect *Nicotiana benthamiana* against insect herbivory and desiccation

Honglin Feng[1] · Lucia Acosta-Gamboa[2] · Lars H. Kruse[3,6] · Jake D. Tracy[4,7] · Seung Ho Chung[1] · Alba Ruth Nava Fereira[5,10] · Sara Shakir[1,8] · Hongxing Xu[1,9] · Garry Sunter[5,10] · Michael A. Gore[2] · Clare L. Casteel[4] · Gaurav D. Moghe[3] · Georg Jander[1]

Received: 5 June 2021 / Accepted: 12 September 2021 / Published online: 29 September 2021

Abstract

Key message ***Nicotiana benthamiana*** **acylsugar acyltransferase (ASAT) is required for protection against desiccation and insect herbivory. Knockout mutations provide a new resource for investigation of plant-aphid and plant-whitefly interactions.**

Abstract *Nicotiana benthamiana* is used extensively as a transient expression platform for functional analysis of genes from other species. Acylsugars, which are produced in the trichomes, are a hypothesized cause of the relatively high insect resistance that is observed in *N. benthamiana.* We characterized the *N. benthamiana* acylsugar profile, bioinformatically identified two acylsugar acyltransferase genes, *ASAT1* and *ASAT2*, and used CRISPR/Cas9 mutagenesis to produce acylsugar-deficient plants for investigation of insect resistance and foliar water loss. Whereas *asat1* mutations reduced accumulation, *asat2* mutations caused almost complete depletion of foliar acylsucroses. Three hemipteran and three lepidopteran herbivores survived, gained weight, and/or reproduced significantly better on *asat2* mutants than on wildtype *N. benthamiana*. Both *asat1* and *asat2* mutations reduced the water content and increased leaf temperature. Our results demonstrate the specific function of two ASAT proteins in *N. benthamiana* acylsugar biosynthesis, insect resistance, and desiccation tolerance. The improved growth of aphids and whiteflies on *asat2* mutants will facilitate the use of *N. benthamiana* as a transient expression platform for the functional analysis of insect effectors and resistance genes from other plant species. Similarly, the absence of acylsugars in *asat2* mutants will enable analysis of acylsugar biosynthesis genes from other Solanaceae by transient expression.

Keywords Acylsugar · Aphid · ASAT · Desiccation · *Nicotiana benthamiana* · Whitefly

✉ Georg Jander
gj32@cornell.edu

[1] Boyce Thompson Institute, Ithaca, NY 14853, USA

[2] Plant Breeding and Genetics Section, School of Integrative Plant Science, Cornell University, Ithaca, NY 14853, USA

[3] Plant Biology Section, School of Integrative Plant Science, Cornell University, Ithaca, NY 14853, USA

[4] Plant-Microbe Biology and Plant Pathology Section, School of Integrative Plant Science, Cornell University, Ithaca, NY 14853, USA

[5] Department of Biology, University of Texas San Antonio, San Antonio, TX 78249, USA

[6] Present Address: Michael Smith Laboratories, University of British Columbia, Vancouver, BC V6T 1Z4, Canada

[7] Present Address: Department of Plant Sciences and Plant Pathology, Montana State University, Bozeman, MT 59717, USA

[8] Present Address: Gembloux Agro-Bio Tech Institute, The University of Liege, Gembloux, Belgium

[9] Present Address: College of Life Science, The Shaanxi Normal University, Xi'an, China

[10] Present Address: Department of Biological Sciences, Northern Illinois University, Dekalb, IL 60115, USA

Introduction

Nicotiana benthamiana, a wild tobacco species that is native to Australia, is commonly employed by plant molecular biologists as platform for investigating plant-virus interactions (Goodin et al. 2008), expression of transgenes using viral and bacterial vectors (Bally et al. 2018), and overproducing proteins and small molecules for subsequent purification (Arntzen 2015; Powell 2015). Although *N. benthamiana* has been used extensively for studying plant-virus and plant-bacterial interactions, it is not a very suitable host for tobacco-feeding generalist herbivores, in particular Hemiptera such as *Myzus persicae* (green peach aphid; Thurston 1961; Hagimori et al. 1993) and *Bemisia tabaci* (whitefly; Simon et al. 2003).

The poor growth of generalist insect herbivores on *N. benthamiana* may be attributed in part to glandular trichomes. These epidermal secretory structures on the leaf surface of ~ 30% of vascular plants (Weinhold and Baldwin 2011; Glas et al. 2012) have been found to play a crucial defensive role in several ways: as a physical obstacle for insect movement (Cardoso 2008), entrapment (Simmons et al. 2004), synthesis of volatiles and defensive metabolites (Laue et al. 2000; Schilmiller et al. 2010; Glas et al. 2012), and production of herbivore-resistance proteins (e.g. T-phylloplanin; Shepherd and Wagner 2007). In addition, glandular trichomes protect plants from abiotic stresses like transpiration water loss and UV irradiation (Karabourniotis et al. 1995).

There are two main types of glandular trichomes on *N. benthamiana* leaves, large swollen-stalk trichomes and small trichomes that are capped by a secretory head with one, two, or four cells. The large trichomes have been shown to secrete phylloplane proteins in *N. tabacum*. The small trichomes, which are the most abundant on tobacco leaf surfaces, secrete exudates, including acylsugars (Wagner et al. 2004; Slocombe et al. 2008).

Acylsugars, generally sucrose or glucose esterified with aliphatic acids of different chain lengths (Fig. 1), are abundant insect-deterrent metabolites (Arrendale et al. 1990; Slocombe et al. 2008; Moghe et al. 2017). Specific acylsugars, which were associated with aphid-resistant *Nicotiana* species, were not detected in susceptible species in this genus (Hagimori et al. 1993). Relative to cultivated tomatoes (*Solanum lycopersicum*), acylsugars found in wild tomatoes (*Solanum pennellii*) were associated with greater resistance against *M. persicae* and *B. tabaci* (Rodriguez et al. 1993; Marchant et al. 2020). The synthetic sucrose octanoate (an analog of *Nicotiana gossei* sugar esters) was effective in the field against Asian citrus psyllids (*Diaphorina citri*), citrus leafminer (*Phyllocnistis citrella*), and a mite complex (including Texas citrus mite, red spider mite, and rust mite) (McKenzie and Puterka 2004; McKenzie et al. 2005).

Although the antimicrobial properties of acylsugars have been studied less extensively, there is evidence that they provide protection against both bacterial and fungal pathogens. *In vitro* assays with acylsugars isolated from several *Nicotiana* species showed *in vitro* antibiotic activity against both gram-positive and gram-negative bacteria (Chortyk et al. 1993). Analysis of natural variation in the acylsugar content of *Nicotiana attenuata* indicated that greater acylsugar abundance provides protection against *Fusarium brachygibbosum* and *Alternaria* sp. (Luu et al. 2017). In the same study, when RNA interference was used to silence the expression of a predicted branched-chain a-ketoacid dehydrogenase gene in *N. attenuata*, acylsugar abundance was reduced by 20–30% and the plants became more susceptible to *F. brachygibbosum* infection. As yet uncharacterized trichome exudates from *S. pennellii*, which likely contain acylsugars, reduced *Oidium neolycopersici* (powdery mildew) infection by suppressing germination of conidia (Nonomura et al. 2009).

Acylsugars and leaf surface lipids more generally may contribute to plant drought tolerance. Transcriptomic studies of drought-tolerant *S. pennellii* populations showed that lipid metabolism genes were among those that are most responsive to drought stress (Gong et al. 2010; Egea et al. 2018), and high acylsugar abundance was associated with drought tolerance (Fobes et al. 1985). Similarly, acylsugar abundance was correlated with drought tolerance in *Solanum chilense* (O'Connell et al. 2007) and *Nicotiana obtusifolia* (Kroumova et al. 2016). Although the mechanism is not completely understood, it has been proposed that the polar lipids reduce the surface tension of adsorbed dew water, thereby allowing the leaves to absorb more condensed water (Fobes et al. 1985).

Recently, enzymes involved in acylsugar biosynthesis have been identified. Four acylsugar acyltransferases (ASATs), *Sl*ASAT1, *Sl*ASAT2, *Sl*ASAT3, and *Sl*ASAT4, have been biochemically characterized in cultivated tomato (Fan et al. 2016). *Sl*ASAT1 catalyzes the first step of sucrose acylation, using sucrose and acyl-CoA to generate monoacylsucroses via pyranose R_4 acylation. *Sl*ASAT2 uses the product of *Sl*ASAT1 and acyl-CoA to generate diacylsucroses. Further, *Sl*ASAT3 uses the diacylsucroses generated by *Sl*ASAT2 to make triacylsucroses by acylating the diacylsucrose five-membered (furanose) ring (Fan et al. 2016). Then, *Sl*ASAT4 (formerly called *Sl*ASAT2), which is specifically expressed in the trichomes, makes tetraacylsucroses by acetylating triacylsucroses using C2-CoA (Schilmiller et al. 2012). The expression, activity, and even the order of ASATs in the biosynthetic pathway varies among different plant species, which likely contributes to the observed trichome chemical diversity (Kim et al. 2012).

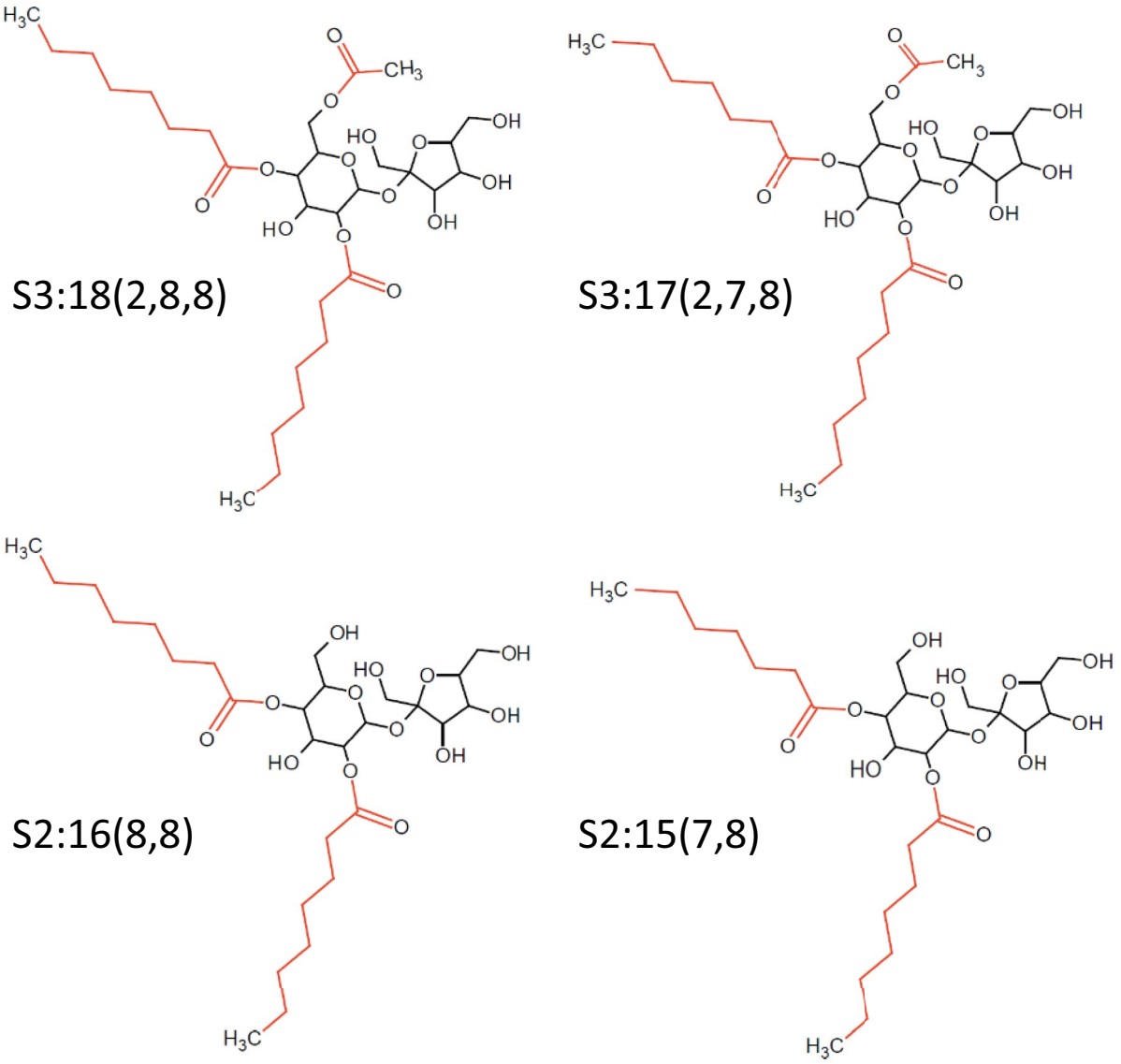

Fig. 1 Predominant acylsugars in *N. benthamiana*. Acylsucroses S3:17(2,7,8), S3:18(2,8,8), S2:16(8,8) and S2:15(7,8) are present in *N. benthamiana*. In the acylsugar structure names, S refers to sucrose, followed by the number of acyl chains, the total length of acyl chains, and the length of each individual chain in parentheses. Although the presence of C2, C7, and C8 chain lengths is confirmed, the specific positions of the acyl chains on the sucrose molecule are hypothesized based on previous observations of acylsugars in *Nicotiana alata* (Moghe et al. 2017), the predicted evolution of the acylsugar biosynthetic pathway, and enzyme promiscuities in the Solanaceae family

Although ASATs have been studied most intensively in cultivated tomato, they also have been biochemically characterized in other *Solanum* (Kim et al. 2012; Fan et al. 2019; Leong et al. 2020) and non-*Solanum* Solanaceae species (Moghe et al. 2017; Nadakuduti et al. 2017). These biochemical analyses, which involved enzyme assays, mass spectrometry, and/or nuclear magnetic resonance techniques, have helped to define the specific acceptor substrates and positions on the sucrose molecule that are being acylated by each of the enzymes. *ASAT*s have been annotated bioinformatically in other available *Nicotiana* genomes (Gaquerel et al. 2013; Van et al. 2017; Egan et al. 2019) but their biochemical characterization is lacking. The goal of the current study was to investigate the previously uncharacterized role of acylsugars in protecting *N. benthamiana* against insect feeding and foliar water loss, as well as to create an insect-susceptible *ASAT* mutant line to facilitate use of *N. benthamiana* for research on plant-insect interactions. Thus, we first bioinformatically identified two *ASAT* genes in *N. benthamiana*, *NbASAT1* and *NbASAT2*. After using CRISPR/Cas9 to create *NbASAT1* and *NbASAT2* mutant lines, we found altered acylsugar profiles, decreased

resistance to six generalist insect herbivores [*M. persicae*, *B. tabaci*, *Macrosiphum euphorbiae* (potato aphid), *Helicoverpa zea* (corn earworm), *Heliothis virescens* (tobacco budworm), and *Trichoplusia ni* (cabbage looper)], and increased foliar water loss.

Results

Identification of ASAT1 and ASAT2 in *N. benthamiana*

Using reciprocal comparisons to confirmed Solanaceae *ASAT* genes (Moghe et al. 2017), we identified three highly homologous sequences in the *N. benthamiana* genome: Niben101Scf02239Ctg025, Niben101Scf22800Ctg001, and Niben101Scf14179Ctg028 (gene identifiers are from annotations at solgenomics.net) (Bombarely et al. 2012). Whereas Niben101Scf02239Ctg025 and Niben101Scf22800Ctg001 were annotated as a full-length coding sequences with strong coverage in available RNAseq datasets, Niben101Scf14179Ctg028 was annotated as a pseudogene because it appears to be a fragment of the predicted cDNA Niben101Scf141790g02010.1, with no coverage in available RNAseq datasets. In a more recent *N. benthamiana* genome assembly (Schiavinato et al. 2019), the Niben101Scf02239Ctg025 and Niben101Scf22800Ctg001 sequences were confirmed, the pseudogene Niben101Scf14179Ctg028 was annotated as part of Niben101Scf02239Ctg025, and there were no additional annotated *ASAT* candidates.

To infer ASAT evolution and function, we constructed a protein phylogenetic tree of previously annotated Solanaceae ASATs, several of which have been biochemically characterized (Fig. 2, S1, S2; Tables S1, S2). In this tree, Niben101Scf02239Ctg025 formed a monophyletic group with other ASATs including the biochemically characterized *Ss*ASAT1, *Pa*ASAT1 and *Hn*ASAT1 (Moghe et al. 2017; Nadakuduti et al. 2017). Therefore, we named Niben101Scf02239Ctg025 as *N. benthamiana* ASAT1 (*Nb*ASAT1). Niben101Scf22800Ctg001 formed a monophyletic group with another set of ASATs, including the biochemically characterized *Ss*ASAT2, *Hn*ASAT2, *Pa*ASAT2 (Moghe et al. 2017; Nadakuduti et al. 2017), *Sn*ASAT1 (Lou et al. 2021), and *Sp*ASAT1 (Fan et al. 2019). Despite the different protein names, all of these orthologous enzymes acylate the R4 position on the pyranose ring of the sugar (Fig. 2). Therefore, given the phylogenetic closeness of *N. benthamiana* to *Salpiglossis sinuata*, *Petunia axillaris* and *Hyoscyamus niger* compared to *Solanum nigrum* and *Solanum pennellii*, we named Niben101Scf22800Ctg001 as *N. benthamiana* ASAT2 (*Nb*ASAT2). Based on the biochemically characterized activities, we predicted the putative functions of the two *Nb*ASATs (Fig. 2). However, some *Nb*ASAT activities still remain uncharacterized.

Generation of ASAT mutants

Using CRISPR/Cas9 coupled with tissue culture, we obtained two independent homozygous mutants for both *NbASAT1* and *NbASAT2*. *asat1-1* has a five-nucleotide deletion at the gRNA3 cutting site and a single-nucleotide insertion at the gRNA2 cutting site, leading to a frameshift between gRNA3 and gRNA2. *asat1-2* has a 318-nucleotide deletion between the gRNA3 and gRNA2 cutting sites (Fig. 3a). *asat2-1* has a single-nucleotide deletion at the gRNA3 cutting site and single-nucleotide insertion at the gRNA2 cutting site, leading to a frameshift between the two sites. *asat2-2* has a 115-nucleotide deletion at the gRNA3 cutting site and a single-nucleotide insertion at the gRNA2 cutting site (Fig. 3b).

Even though *ASAT1* and *ASAT2* are located on different scaffolds in the *N. benthamiana* genome assembly (Schiavinato et al. 2019), we were not able to find homozygous *asat1 asat2* double mutants among 40 F2 progeny from crosses between *asat1* and *asat2* plants. Similarly, when we transformed *N. benthamiana* in tissue culture with gRNA targeting both *ASAT1* and *ASAT2*, simultaneously or sequentially, we identified each individual knockout mutation, but no homozygous double mutants. Although we cannot completely rule out other scenarios, it is possible that *asat1 asat2* double mutations are deleterious or lethal for *N. benthamiana.*

ASAT2 knockout depletes acylsugar biosynthesis

In the LC/MS profile of *N. benthamiana* leaf surface washes, we characterized twelve mass features as acylsucroses based on their characteristic peaks and neutral losses. Those twelve *m/z* ratios included 383.12, 467. 21, 509.22, 555.23, 593.32, 621.31, 625.31, 635.32, 639.32, 667.32, 671.30, 681.34 (Fig. S3a). In negative electron spray ionization mode, the characteristic peak features included *m/z* of 341.11 for sucrose, 509.22 for sucrose + C2 + C8, 467.21 for sucrose + C8, 495.21 for sucrose + C7, and 383.12 for sucrose + C2; the neutral loss peaks included mass for 126.10 for C8 (acyl-chain with 8 carbons), 129.09 for C7 + H_2O, and 59.01 for C2 + H_2O (Fig. S3b). Based on their MS/MS peak features, retention times and relative abundances, we predicted that the identified mass features are mainly derived from two acylsucroses as formate or chloride adducts, pathway intermediates, and/or resulted from in-source fragmentation. We named the two acylsucroses S3:17(2,7,8) and S3:18(2,8,8). In this nomenclature, "S" refers to the sucrose backbone, "3:18" indicates three acyl chains with total eighteen

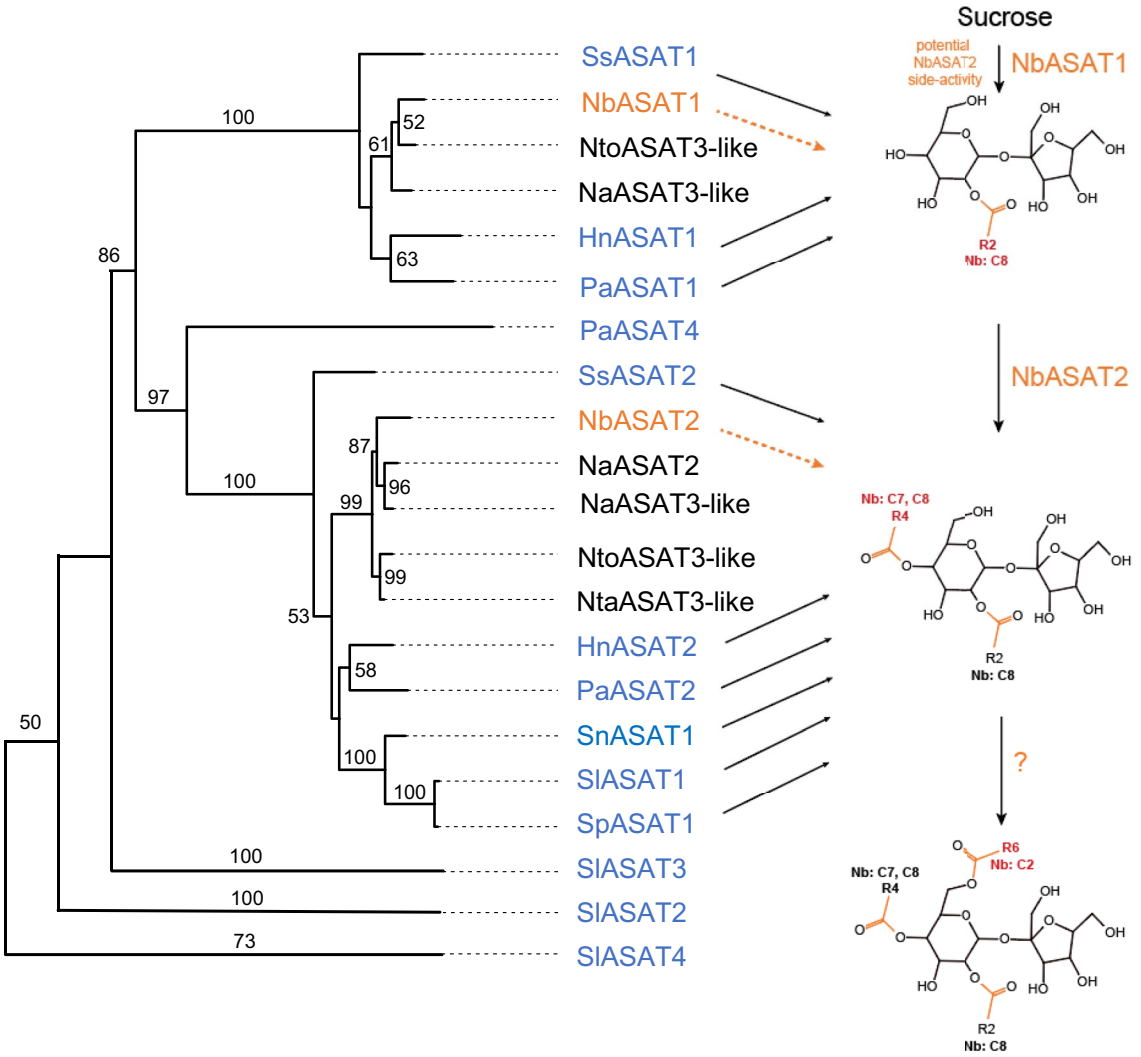

Fig. 2 ASAT phylogenetic tree and predicted enzymatic functions. The evolutionary history of ASATs in the Solanaceae (Tables S1 and S2) was inferred using the Maximum Likelihood method in RAxML. Presented is a subtree of a larger tree that includes all annotated ASATs (Figure S1). The branch labels indicate the percentage of trees in which the associated taxa clustered together (bootstrap of 1000). Only values greater than 50 are presented. The two predicted *N. benthamiana* ASATs are highlighted in orange and ASATs that were previously chemically characterized are highlighted in blue. The position of the R6 acylation is based on positive mode fragmentation results in *N. alata* (Moghe et al. 2017: Fig. 1–Figure supplement 4), which found all acylation, including an acetylation on the pyranose ring. R2, R4, R6 refer to the positions on the pyranose. Arrows from characterized enzymes point to the classes of structures that are produced by these reactions. Dashed arrows indicate that the acylation positions of these two *N. benthamiana* enzymes are predicted based on previously experimentally identified acylation positions of orthologous enzymes (solid arrows). *SS Salpiglossis sinuata*, *Nb Nicotiana benthamiana*, *Nto Nicotiana tomentosiformis*, *Na Nicotiana attenuata*, *Hn Hyoscyamus niger*, *Pa Petunia axillaris*, *Nta Nicotiana tabacum*, *Sn Solanum nigrum*, *Sl Solanum lycopersicum*, *Sp Solanum pennellii*

carbons, and the length of each acyl chain is shown in parentheses (Fig. 1; S3a).

In wildtype plants, S3:18(2,8,8) is the dominant acylsucrose, whereas S3:17(2,7,8) has relatively low abundance (Fig. 4). S2:16(8,8) and S2:15(7,8), which may be biosynthetic pathway intermediates for S3:18(2,8,8) and S3:17(2,7,8), respectively, are present at lower levels. Compared to wildtype *N. benthamiana*, both *asat2-1* and *asat2-2* were almost completely depleted in both S3:17(2,7,8) and S3:18(2,8,8), as well as in the two predicted biosynthetic intermediates S2:15(7,8) and S2:16(8,8). For *asat1-1* and *asat1-2*, the detected acylsucroses were less abundant and significantly reduced only in *asat1-1* (Fig. 4). Although acylsugar content was reduced in the *ASAT* mutants, the structure and abundance of trichomes on the leaf surface were not visibly changed (Fig. S4).

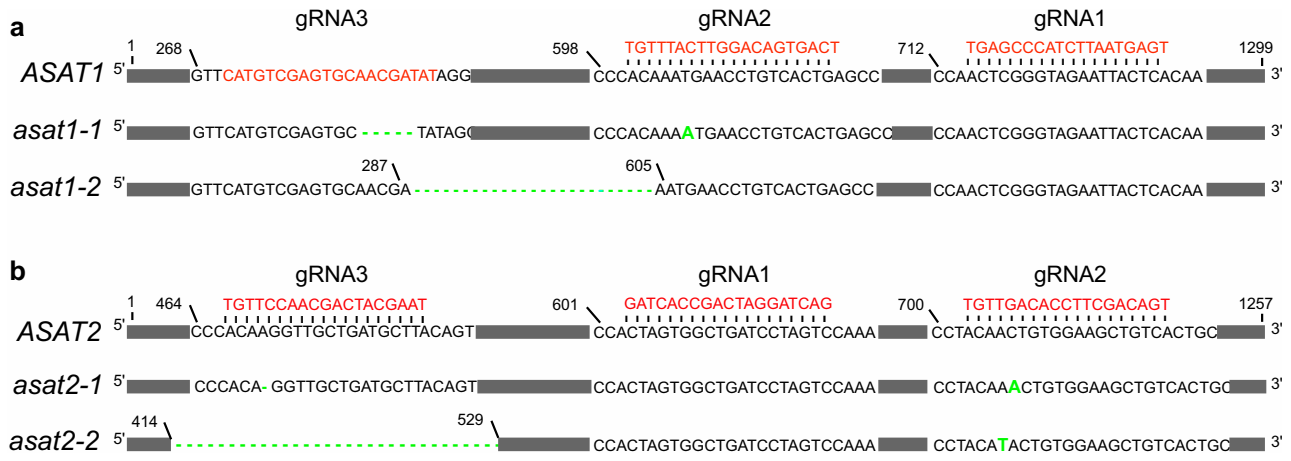

Fig. 3 *Nicotiana benthamiana* ASAT mutations produced with CRISPR/Cas9. Three gRNAs (sequences shown in red) were designed to edit either *ASAT1* or *ASAT2*. Whereas gRNA3 for ASAT1 is on the sense strand, the other gRNAs are on the antisense strand. For both *ASAT1* and *ASAT2*, we obtained two independent mutations resulting from the corresponding gRNA2 and gRNA3. Single-base mutations and deletions are shown in green. **a** *asat1-1* has a five-nucleotide deletion at gRNA3 and a single-nucleotide insertion at gRNA2. *asat1-2* has a 318-nucleotide deletion between the gRNA3 and gRNA2 cutting sites. **b** *asat2-1* has a single-nucleotide deletion at gRNA3 and single-nucleotide insertion at gRNA2 leading to a translation frame shift between the two mutations. *asat2-2* has a 115-nucleotide deletion at gRNA3 and a single-nucleotide insertion leading to a translation frame shift at gRNA2

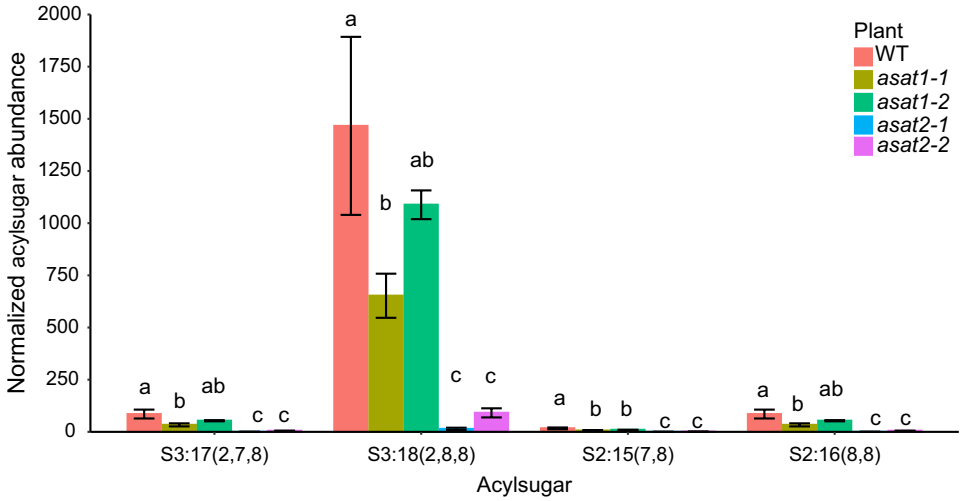

Fig. 4 Abundance of two *Nicotiana benthamiana* acylsugars (S2:17(2,7,8) and S2:18(2,8,8)), and two likely pathway intermediates/fragmentations (S2:15(7,8) and S2:16(8,8)). Acyl sugar LC/MS peak areas were normalized relative to the peak area of Telmisartan, which was added as an internal control, and then to the leaf dry weight (per gram). Error bars represent standard errors from measurements of three plants of each genotype. Significant differences for each acylsugar between different genotypes were tested using one-way ANOVA followed by a Duncan's post hoc test ($p < 0.05$). Differences between groups are denoted with letters

Insect performance is improved on ASAT2 mutant lines

To test the role of acylsugars in protecting *N. benthamiana* against insect pests, we started with synchronized first-instar *M. persicae* to monitor aphid survival and growth over time. Significant improvements in aphid survivorship were observed as early as at 2 days post-feeding ($p < 0.001$) on the *asat2-1* and *asat2-2* mutants and increased until the end of the 5-day monitoring period ($p < 0.001$) (Fig. 5a; Table S3). After 5 days of feeding, surviving aphids on both *asat1* and *asat2* plants were larger than those on wildtype plants (Fig. 5b). When we measured progeny production by five adult aphids over a period of seven days, an average of more than 200 nymphs were produced on the *asat2* mutants, significantly more than the number of nymphs produced on either wildtype or *asat1* mutants ($p < 0.05$, Fig. 5c). In aphid choice assays, a preference for *asat2-1* and *asat2-2*

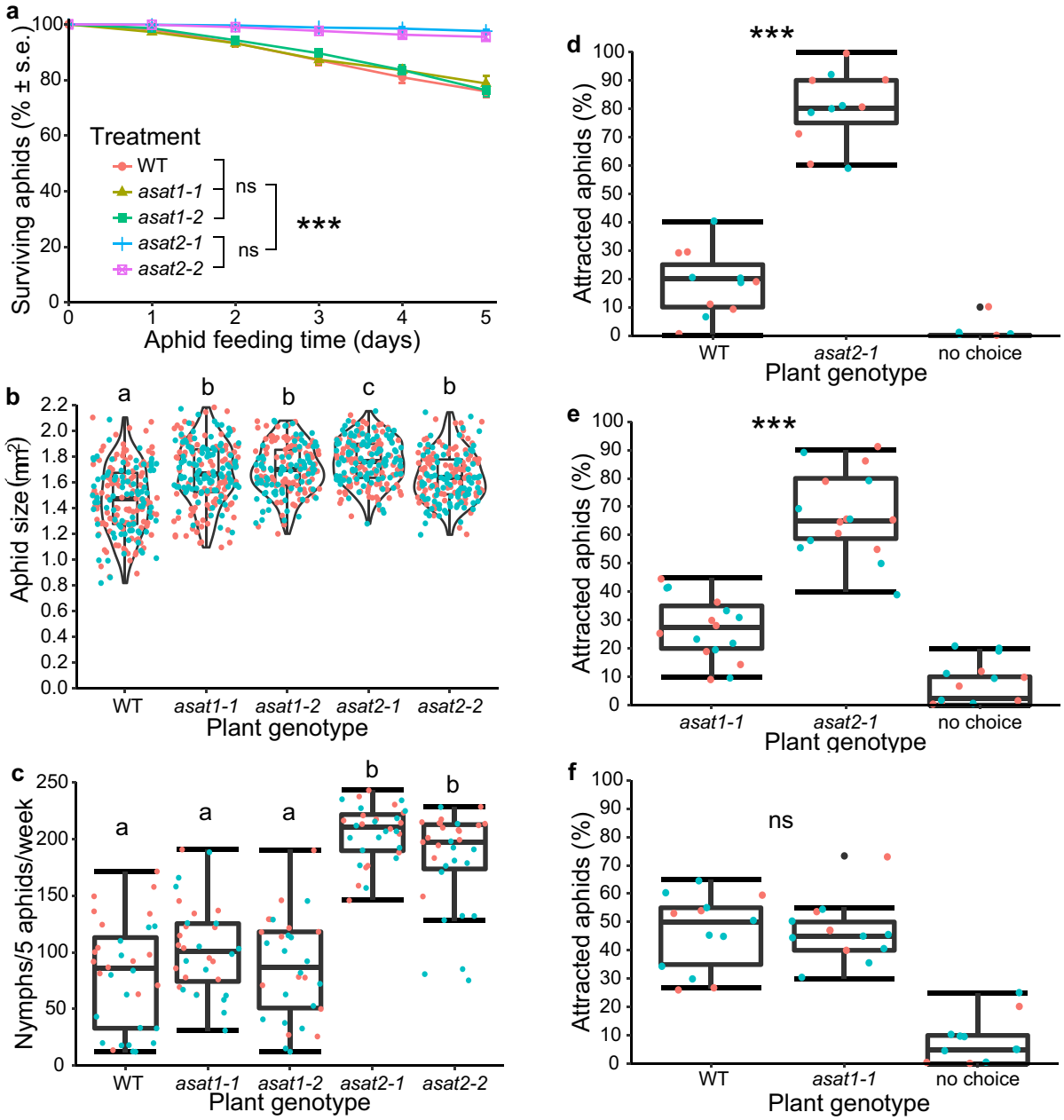

Fig. 5 *Myzus persicae* bioassays with wildtype (WT), *asat1*, and *asat2 N. benthamiana*. Data shown in all panels were combined from two independent experiments, which are shown in color orange and cyan in panels B–F. **a** Survival over 5 days of nymphs placed onto mutant and wildtype *N. benthamiana*. Significant differences are indicated for the 5-day time point: ns: not significant, ***$p < 0.001$, mean +/− s.e. of n = 15–16. Significant differences were tested using one-way ANOVA with a fixed factor of genotypes and a block effect of experiment followed by a Bonferroni post hoc test for multiple comparisons. Full statistical data for all time points are in Table S4. **b** Aphid growth, as measured by body size after 5 days feeding on *N. benthamiana*. **c** Aphid reproduction, as measured by the number of nymphs that were produced by five aphids in one week. Significant differences between different groups ($p < 0.05$) were determined using ANOVA with a fixed factor of genotypes and a block effect of experiment followed by a Duncan's post hoc test and are indicated by lowercase letters above each group in panels B and C. **d–f** Aphid choice among detached leaves of each plant genotype, significant differences between genotypes were assessed using Chi-squared tests, ***$p < 0.001$; ns: no significant difference; no choice: aphids were elsewhere in the Petri dish and not on a leaf. The box plots show the median, interquartile range, maximum and minimum after removal of outliers, and the individual data points

leaves was consistently observed in any pairwise combination with wildtype, *asat1-1*, and *asat1-2* leaves ($p < 0.001$, *Chi-squared* test, Fig. 5d, e; S5). No *M. persicae* preference was observed between wildtype *N. benthamiana* and *asat1* mutants ($p > 0.05$, Fig. 5f; S5).

When aphid colonies were allowed to grow long-term on *asat2-1* mutant and wildtype *N. benthamiana* in the same cage, there were many more aphids on the mutant plants (Fig. S6a,b), likely resulting from a combination of host plant choice and increased growth on the *asat2-1* mutant. It is noteworthy that, on the *asat2-1* mutant plants, aphids were feeding on the more nutritious younger leaves, which tend to be better-defended in plants. By contrast, on wildtype *N. benthamiana* aphids were only were able to feed on older, senescing leaves and were primarily on the abaxial surface. Consistent with the increased aphid presence, growth of the *asat2-1* mutant plants was visibly reduced relative to wildtype *N. benthamiana* (Fig. S6b). Given the almost identical phenotypes of *asat2-1* and *asat2-2* mutants, subsequent insect assays were conducted with T2 progeny of the *asat2-1* line.

Significantly increased *M. euphorbiae* survival was observed after 24 h on *asat2-1* compared to wildtype ($p < 0.001$, Fig. 6a). Additionally, significantly more nymphs were produced by adult *M. euphorbiae* in the course of 24 h on *asat2-1* than on wildtype ($p < 0.05$, Fig. 6b). In choice assays, *M. euphorbiae* preferentially chose *asat2-1* leaves over wildtype leaves ($p < 0.001$, Fig. 6c). Whereas we were not able to establish an *M. euphorbiae* colony on wildtype *N. benthamiana*, the aphids readily formed colonies on the *asat2-1* mutant plants (Fig. 6d).

Survival of *B. tabaci* adults was greatly increased on the *asat2-1* mutant relative to wildtype *N. benthamiana* (Fig. 6e). Moreover, whiteflies laid significantly fewer eggs on wildtype than on *asat2-1* mutant plants over three days (Fig. 6f). Dead adult whiteflies were observed on wildtype plants (Fig. S7a), and it was not possible to establish a reproducing colony. By contrast, after 23 days of feeding, whiteflies of different life stages were observed on *asat2-1* mutant plants (Fig. S7b–d). In choice assays with mutant and wildtype plants in the same cage, whiteflies preferentially settled on *asat2-1* plants (72%) over wildtype (26%) in a 24-h experiment (Fig. 6g). Notably, after 24 h, all whiteflies on *asat2-1* were alive, whereas about half of the whiteflies that had settled on the wildtype plants were dead (Fig. 6f).

To determine whether depletion of acylsugars in *ASAT2* mutants improves the performance of generalist lepidopteran herbivores on *N. benthamiana*, we conducted experiments with *H. zea*, *H. virescens*, and *T. ni*. When neonates were placed on the leaves of wildtype or *asat2-1* mutant, no *H. zea* caterpillars were recovered (Fig. 7a). Survivorship of *H. virescens* and *T. ni* larvae on *N. benthamiana* was low, and the mass of the surviving larvae after ten days was not significantly increased on the mutant relative to wildtype (Fig. 7b, c). Due to the low survival of neonates, we repeated the caterpillar bioassay using five-day-old larvae that had been reared on artificial diet. Almost all *H. zea* and *H. virescens* larvae survived for seven days on wildtype and *asat2-1* mutant plants, and survival of *T. ni* caterpillars was higher on *asat2-1* than on wildtype plants (Fig. 7d–f). The relative growth rates of surviving *H. zea*, *H. virescens*, and *T. ni* larvae were higher on the *asat2-1* mutant by 35, 47, and 99%, respectively, than on wildtype plants (Fig. 7d–f).

Water loss is greater in *asat2* mutant plants than in wildtype

While conducting aphid choice assays with detached leaves (Figs. 5d–f and 6c), we noticed that the mutant leaves dried out faster than wildtype leaves. This effect was quantified using detached-leaf assays, in which *asat2* leaves lost significantly more water over 24 h than leaves from either wildtype or *asat1* mutant (Fig. 8a; S8a). Using hyperspectral imaging, we determined that the leaf water content of intact plants, as measured by the water band index (WBI), was significantly lower in *asat2* mutants than in wildtype (Fig. 8b; S8b). Although the *asat1* mutants did not lose water faster than wildtype in detached leaf assays (Fig. 8a), the leaf water content in *asat1* mutants was significantly lower than in wildtype (Fig. 8b; S8b). Measurement of leaf temperature by thermal imaging showed that, consistent with the reduced leaf water content, the leaf temperature of the acylsugar mutants was significantly higher than that of wildtype plants (Fig. 8c; S8c).

Discussion

Previous studies with other Solanaceae species (Moghe et al. 2017; Nadakuduti et al. 2017; Fan et al. 2019; Leong et al. 2020) identified more than a dozen BAHD acyltransferases involved in acylsugar biosynthesis (Fig. 2). Using the Solanaceae phylogeny as a guide, we identified two BAHD genes, *NbASAT1* and *NbASAT2* that are orthologs of the non-*Solanum ASAT1* and *ASAT2* in *Petunia axillaris*, *Salpiglossis sinuata*, and *Hyoscyamus niger*. The ortholog of the *ASAT3* gene in these three species appeared to be a fragmented pseudogene in the *N. benthamiana* genome (Table S2). Nonetheless, the *N. benthamiana* genome has at least 124 genes encoding proteins with a BAHD acyltransferase domain (PFam: PF02458). Thus, it is possible that additional BAHDs are involved in *N. benthamiana* acylsugar biosynthesis, for instance catalyzing the acetylation reaction to make triacylsucroses (Fig. 2). Other enzyme classes also contribute to acylsugar biosynthesis. Knockdown of *E1-β branched-chain α-keto*

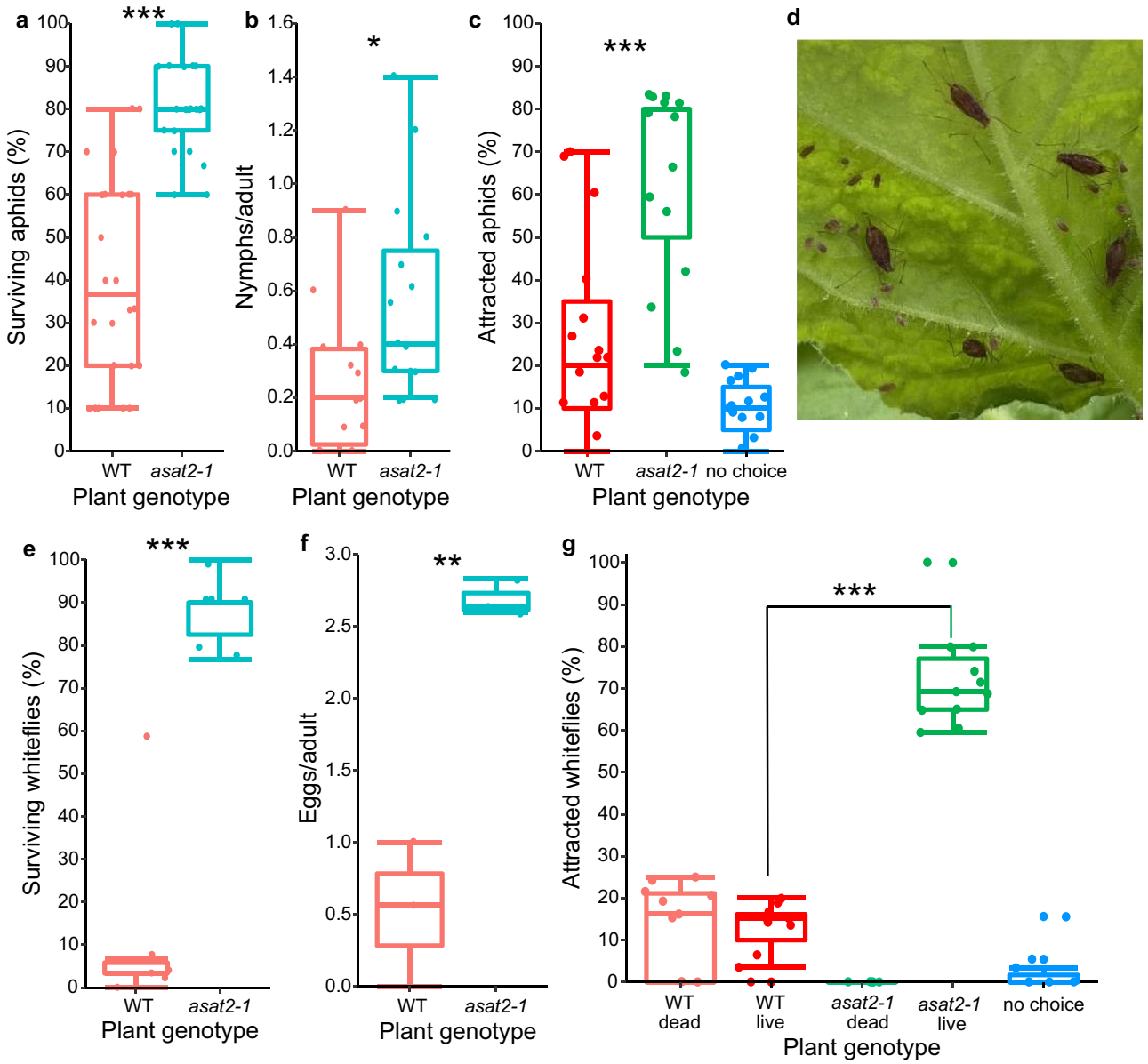

Fig. 6 Potato aphid and whitefly bioassays on *asat2-1* and wildtype (WT) *N. benthamiana*. **a**–**d** potato aphid (*M. euphorbiae*) bioassays. **a** aphid survival in 24 h (n = 15). **b** aphid reproduction in 24 h (n = 15). **c** aphid choices between detached leaves of each plant genotype (n = 15). **d** An established *M. euphorbiae* colony on an *N. benthamiana asat2-1* leaf. **e**–**g** whitefly bioassays. **e** whitefly survival in 3 days (n = 6). **f** whitefly reproduction measured as number of eggs produced per adults in 3 days (n = 3). **g** whitefly choices between plants of each genotype (n = 3 for 4 independent experiments). Significantly differences were tested using independent *t*-tests for aphid and whitefly survival and reproduction data. Chi-squared tests were used for aphid and whitefly choice assays. $*p < 0.05$, $**p < 0.01$, $***p < 0.001$; no choice: insects were not on a leaf at the end of the experiment. The box plots show the median, interquartile range, maximum and minimum after removal of outliers, and the individual data points

acid dehydrogenase significantly reduced acylsugars in *N. benthamiana* (Slocombe et al. 2008). Additionally, *Isopropylmalate Synthase 3* in cultivated and wild tomatoes (Ning et al. 2015) and *Acyl-Sucrose Fructo-Furanosidase 1* in wild tomato (Leong et al. 2019) encode enzymes that are involved in determining acylsugar composition. Further studies will be needed to characterize additional genes involved in *N. benthamiana* acylsugar biosynthesis.

Tomato *ASAT* genes were identified at least partly due to their specific expression in the tip cells of secretory trichomes, where the plants produce acylsugars (Schilmiller et al. 2012; Schilmiller et al. 2015). Although it is probable

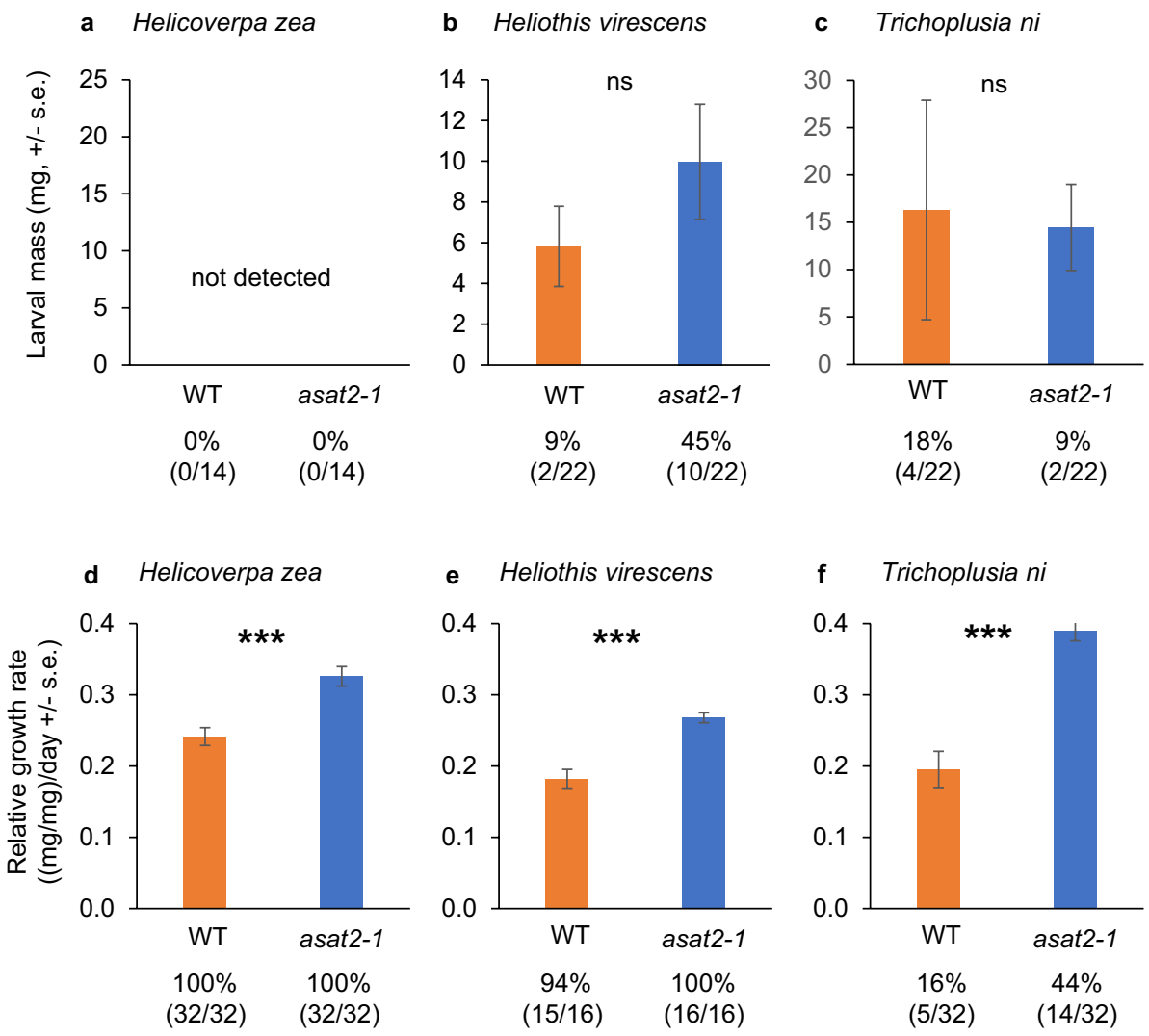

Fig. 7 Caterpillar bioassays on wildtype (WT) and *asat2-1* mutant *N. benthamiana*. **a**–**c** Larval mass of surviving *Helicoverpa zea*, *Heliothis virescens*, and *Trichoplusia ni* 10 days after being placed on plants as neonates. **d**–**f** Relative growth rate of surviving *H. zea*, *H. virescens*, and *T. ni* on wildtype and *asat2-1* plants. Insects were raised for five days on artificial diet, prior to 7 days of feeding on *N. benthamiana*. Percent survival (number of surviving insects/number of total insects) is shown below each figure. Mean +/− s.e. ,***$p < 0.001$, *t*-test; ns: no significant difference ($p > 0.05$)

that *N. benthamiana ASAT* genes are similarly expressed in the trichome tips, this will require experimental verification, for instance with the expression of GFP fusion proteins in transgenic plants. Given the short-term nature of our insect feeding and water loss assays, they likely reflect the effects of constitutive acylsugar abundance on the leaves. Thus, we do not know whether there is stress-induced production of acylsugars, in *N. benthamiana.* More research also is required to investigate the tissue-specific abundance of acylsugars in this species.

Acylsugars can be categorized as sucrose or glucose esters based on the sugar cores, which are decorated with varying numbers or lengths of acyl chains (Kim et al. 2012). Whereas some wild tomatoes produce a mixture of acylsucroses and acylglucoses, we observed only acylsucroses (Figs. 1 , 4), consistent with previous identification of these compounds in *N. benthamiana* (Matsuzaki et al. 1989; Matsuzaki et al. 1992; Hagimori et al. 1993; Slocombe et al. 2008). Nevertheless, it has been reported that *N. benthamiana* produces acylglucoses, although in lower abundance than acylsucroses (Hagimori et al. 1993), and one acylglucose structure has been proposed (Matsuzaki et al. 1992). Our failure to detect acylglucoses may be explained by the use of different growth conditions, plant stage, and/or the detection methods. Whereas we used ~ 1-month-old plants and LC/MS, Matsuzaki et al. (1992) used ~ 3-month-old plants and GC/MS to detect acylglucoses in *N. benthamiana*. Significant within-species acylsugar variation has been observed in

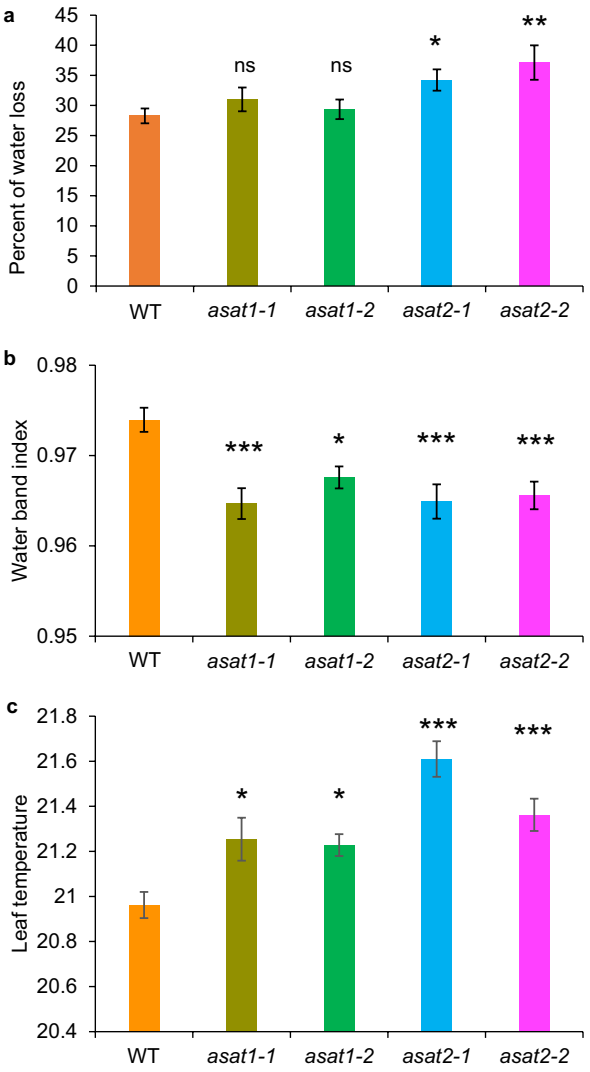

Fig. 8 Water loss and leaf temperature of wildtype (WT), *asat1*, and *asat2 Nicotiana benthamiana.* **a** Percent of water loss from detached leaves in 24 h, mean +/− s.e. of n = 15. **b** Leaf water content measured by the water band index from hyperspectral imaging, mean +/− s.e. of n = 20. **c** Leaf temperatures from leaves of different plant genotypes, mean +/− s.e. of n = 20. *ns* no significant difference, $*p < 0.05$, $**p < 0.01$, $***p < 0.001$, Dunnett's test relative to wildtype control

Solanum habrochaites (Kim et al. 2012; Landis et al. 2021). Thus, similar variation among *N. benthamiana* isolates also could explain differences in the acylsugar structures that were found in our study and previous ones.

Acylsugar abundance was reduced to a greater extent in *N. benthamiana asat2* than in *asat1* mutants (Fig. 4). This suggests that: (i) *Nb*ASAT1 and *Nb*ASAT2 have similar functions in the biochemical pathway, but *NbASAT2* had higher abundance or enzymatic activity, or (ii) *Nb*ASAT2 functions upstream of *Nb*ASAT1 in the acylsugar biosynthesis pathway, but partially complements *Nb*ASAT1 activity. In the ASAT phylogenetic tree (Fig. 2), *Nb*ASAT2 is closely related to some biochemically characterized ASAT1 proteins in other Solanaceae species, including the *Sp*ASAT1 and *Sl*ASAT1 from *Solanum* species. The latter ASAT1s use sucrose as the substrate while their orthologs in non-*Solanum* species, namely *Salpiglossis sinuata*, *Hyoscyamus niger*, and *Petunia axillaris,* show ASAT2 activity and use mono-acylsucroses as substrates. We thus previously hypothesized (Moghe et al. 2017) that the non-*Solanum* ASAT2 enzymes may display promiscuous activity towards the ASAT1 substrate (sucrose) in some species. This promiscuous activity may have been selected for in *Solanum*, leading to ASAT2 becoming ASAT1 in the *Solanum* genus. Since there is greater loss of acylsugars in *NbASAT2* knockouts than in *NbASAT1* knockouts, we speculate that NbASAT2 has some promiscuous activity towards the NbASAT1 substrate (sucrose), enabling it to partially complement the NbASAT1 phenotype. If this hypothesis is true, it may flag a transition stage for the non-*Solanum* ASAT2s. Alternatively, the observations may indicate independent *Nicotiana*-specific evolution of the ASAT1 and ASAT2 functions. Based on previous knowledge of BAHD activities (Moghe et al. 2017), we postulate that S2:15 (7,8) and S2:16 (8,8) are produced by *Nb*ASAT1 and *Nb*ASAT2 (Fig. 2), whereas the acetylation is carried out by another unrelated BAHD enzyme – not unlike the distantly related *Sl*ASAT4 and *Salpiglossis sinuata* ASAT5 (Schilmiller et al. 2015; Moghe et al. 2017). Although it is not known whether *N. benthamiana* ASATs are monomeric or multimeric, BAHD acyltransferases generally are monomeric enzymes (D'Auria 2006), suggesting that formation of ASAT1-ASAT2 heterodimers is unlikely to affect the observed phenotypes.

The observed role of acylsugars in protecting against desiccation (Fig. 8; S8) is consistent with reports from other Solanaceae (Fobes et al. 1985; O'Connell et al. 2007; Kroumova et al. 2016), though this has not previously been verified with isogenic mutant and wildtype plants. In *N. benthamiana*, the drought-protective function of acylsugars is likely an adaptation to the seasonally arid native habitat in northwestern Australia (Goodin et al. 2008; The Australasian Virtual Herbarium, https://avh.ala.org.au). Relative to *asat1* mutants, the lower acylsugar content of *asat2* mutants (Fig. 4), resulted in more rapid water loss in detached leaves (Fig. 8a; S8a). Despite the only partial decrease in the acylsugar content of *asat1* mutants, the decreases in water content and increases in leaf temperature of intact plants were similar to those of *asat2* mutants (Fig. 8b, c; S8b, c). However, we cannot rule out the possibility that loss of ASAT1 activity has direct or indirect effects on other metabolites that affect water loss in *N. benthamiana* leaves.

Acylsugars with C_{7-12} chains have been shown to be the most toxic sugar esters for small phloem-feeding Hemiptera such as aphids, Asian citrus psyllids, and whiteflies

(Chortyk et al. 1996; McKenzie and Puterka 2004; Song et al. 2006). Synthetic acylsucroses with di-heptanoic acid (C7), di-octanoic acid (C8), and di-nonanoic acid (C9) acyl groups showed the highest mortality in bioassays with *M. persicae* and *B. tabaci* (Chortyk et al. 1996; McKenzie and Puterka 2004; Song et al. 2006). *Nicotiana gossei*, a tobacco species that produces mainly C7-C8 acyl group acylsugars, has a high level of insect resistance compared to close relatives with acylsugar profiles that are not dominated by those with C7-C12 acyl groups (Thurston 1961; Kroumova and Wagner 2003). In *N. benthamiana*, the two most abundant acylsugars that we found contain C7 and predominantly C8 acyl groups, which is consistent with previous findings of mainly 5- and 6-methyl heptanoate (C8) in *N. benthamiana* (Kroumova and Wagner 2003; Slocombe et al. 2008) and *N. alata* (Moghe et al. 2017). The almost complete depletion of acylsugars in our *asat2* mutants improved both hemipteran and lepidopteran performance, suggesting that acylsugars with C8 acyl groups are providing insect resistance in *N. benthamiana*.

We cannot rule out the possibility of secondary effects that might also influence insect performance on acylsugar-depleted *N. benthamiana*. Specialized metabolites in other plants, for instance glucosinolates in *Arabidopsis thaliana* (Clay et al. 2009) and benzoxazinoids in *Zea mays* (Meihls et al. 2013), regulate callose deposition as a secondary defense response. It is not known whether acylsugars contribute to the regulation of other defense responses in *N. benthamiana.* The observation of numerous dead whiteflies on wildtype *N. benthamiana* plants in choice assays (Fig. 6g), despite the option of moving to presumably more desirable *asat2-1* mutant plants in the same cage, suggests that the acylsugars' stickiness also plays a role in plant defense by immobilizing the insects. Both altered leaf turgor and leaf temperature (Fig. 8b, c) could affect insect feeding behavior and growth rate, though the specific effects on the six tested insect species cannot be determined without further research.

Although *H. zea*, *H. virescens*, and *T. ni* larvae grow well on cultivated tobacco, neonate larvae had a low survival rate on both wildtype and *asat2-1 N. benthamiana* (Fig. 7a–c). There was a higher survival rate with five-day-old larvae of the three tested species, which all grew significantly better on *asat2-1* mutants than on wildtype *N. benthamiana* (Fig. 7d–f). Thus, *N. benthamiana* acylsugars likely provide at least some protection against lepidopteran pests. However, the high mortality of neonate larvae on *asat2-1* plants suggests that either residual acylsugars or as yet unknown resistance mechanisms in *N. benthamiana* can provide protection. Additional mutations that decrease insect resistance, perhaps regulatory genes such as *COI1* or genes affecting the production of other specialized metabolites, will be necessary to facilitate *N. benthamiana* experiments with *H. zea*, *H. virescens*, *T. ni*, and other commonly studied lepidopteran species.

The high mortality of hemipteran pests such as *M. persicae* and *B. tabaci* on wildtype *N. benthamiana* (Figs. 5, 6) makes it challenging to interpret insect bioassays involving the transient expression of heterologous genes. Our knockout of acylsugar biosynthesis is an important step toward making the already excellent *N. benthamiana* model system (Goodin et al. 2008; Bally et al. 2018) more suitable for studying plant-insect interactions. Future plant-insect interactions research using *asat2* mutant plants may include: (i) functional analysis of additional *N. benthamiana* genes in the *asat2* mutant background by CRISPR/Cas9 mutagenesis using a newly developed virus-mediated gRNA delivery system (Ellison et al. 2020), (ii) transient expression assays to test the function of both insect-produced elicitors and insect-defensive genes from other plant species in *N. benthamiana asat2* mutants (Bos et al. 2010; Casteel et al. 2014; Elzinga et al. 2014; Rodriguez et al. 2014), and (iii) virus-induced gene silencing (VIGS) to down-regulate gene expression in insects feeding on *N. benthamiana* (Feng and Jander 2021). Furthermore, the almost complete absence of acylsugars in the *asat2* mutant lines, coupled with the facile *Agrobacterium* and virus-mediated transient gene expression systems that are available for *N. benthamiana*, will make these mutants a suitable platform for the functional analysis of ASATs from other Solanaceae.

Materials and methods

Insect and plant cultures

A tobacco-adapted red strain of *M. persicae* (Ramsey et al. 2007; Ramsey et al. 2014) was maintained on *N. tabacum* plants in a growth room at 23 °C with a 16:8 h light:dark photoperiod. A colony of *B. tabaci* MEAM1 were provided by Jane Polston (University of Florida) and was maintained on tobacco (*Nicotiana tabacum*). *Macrosiphum euphorbiae* was obtained from Isgouhi Kaloshian (UC Riverside) and was maintained on tomato (*Solanum lycopersicum*) cv. Moneymaker. Eggs of *H. zea*, *H. virescens*, and *T. ni* were purchased from Benzon Research (www.benzonresearch.com). *Nicotiana benthamiana* wild type and mutant plants for aphid experiments, caterpillar experiments were maintained at 23 °C and a 16:8 h light:dark photoperiod in a Conviron (Winnipeg, Canada) growth chamber and, for seed production, in a greenhouse at 27/24 °C (day/night) with ambient light conditions. Wild type and mutant *N. benthamiana* plants for whitefly choice and no-choice assays were maintained at 26 °C and a 16:8 h light:dark photoperiod in a growth room.

Identification of ASAT1 and ASAT2 orthologs in *N. benthamiana*

To identify ASAT1 and ASAT2 orthologs in *N. benthamiana*, protein sequences of *Salpiglossis sinuata* and *Solanum lycopersicum* ASAT1 and ASAT2 (Moghe et al. 2017) were compared to predicted proteins encoded by the *N. benthamiana* genome. Sequences with > 67 % identity were selected as potential ASAT1 and ASAT2 candidates and nucleotide sequences were obtained from the Solanaceae Genomics Network (www.solgenomics.net). The candidate *ASAT* sequences were subsequently confirmed by comparison to the most recently published *N. benthamiana* genome assembly (Schiavinato et al. 2019). To verify the nucleotide sequences of *N. benthamiana ASAT1* and *ASAT2*, the genes were amplified with ASAT1F/ASAT1R and ASAT2F/ASAT2R primers (Table S4) from genomic DNA. Amplified fragments were cloned in pDONOR™207 (ThermoFisher Scientific, US) and were sequenced in their entirety using Sanger sequencing, which showed no differences to the published *N. benthamiana* genome.

Phylogenetic analysis of N. benthamiana *ASATs*.

A protein phylogenetic tree of previously annotated Solanaceae ASATs (Fig. 2, S1, S2; Tables S1, S2) was constructed using maximum likelihood method. Briefly, the ASAT protein sequences were aligned in ClustalW (Thompson et al. 1994). Then the alignment was improved by removing spurious sequences and poorly aligned regions (gap threshold at 0.25) using TrimAL v1.4 (Capella-Gutierrez et al. 2009). Finally, an unrooted maximum likelihood tree was generated using the improved alignment with a bootstrap of 1000 in RAxML v8.2.12 (Stamatakis, 2014). The tree was visualized and presented using FigTree v1.4.4 (http://tree.bio.ed.ac.uk).

sgRNA design and plasmid cloning

Single-guide RNAs (sgRNA) targeting *ASAT1* and *ASAT2* were designed based on the coding regions using CRISPR-P v2.0 (Liu et al. 2017) and CRISPRdirect (https://crispr.dbcls.jp/), based on cleavage efficiency and lack of potential off-target sites in the *N. benthamiana* genome. Additionally, only sgRNAs with > 40% GC content were selected.

Three Cas9/gRNA constructs each were constructed for *ASAT1* and *ASAT2* following a previously developed CRISPR/Cas9 system (Jacobs et al. 2015). Four segments of DNA were prepared with 20-bp overlaps on their ends. (1) ssDNA gRNA oligonucleotides targeting either the sense or antisense sequence of target genes were designed as: sense oligo TCAAGCGAACCAGTAGGCTT-GN19-GTTTTAGAGCTAGAAATAGC, and antisense oligo GCT ATTTCTAGCTCTAAAAC-N19C-AAGCCTACTGGT TCGCTTGA (the gRNA sequences are shown in Fig. 3; Table S4), and synthesized by Integrated DNA Technologies (www.idtdna.com). One µl of each 100 µM oligo was added to 500 µl 1x NEB buffer 2 (New England Biolabs, www.neb.com). (2) The p201N:Cas9 plasmid was linearized by digestion with *Spe*1 (www.neb.com) in 1x buffer 4 at 37 °C for 2 h, followed by column purification and a second digestion with *Swa*l in 1x buffer 3.1 at 25 °C for 2 h. Complete plasmid digestion was confirmed on a 0.8 % agarose gel. (3) The MtU6 promoter and (4) Scaffold DNAs were PCR-amplified from the pUC gRNA Shuttle plasmid (Jacobs et al. 2015) using the primers *Swa*l_MtU6F/MtU6R and ScaffoldF/Spe_ScaffoldR, respectively (Table S4). The PCR reactions were performed with a high-fidelity polymerase (2× Kapa master mix; www.sigmaaldrich.com) using the program: 95 °C for 3 min followed by 31 cycles of 98 °C for 20 s, 60 °C for 30 s, 72 °C for 30 s, and a final extension of 72 °C for 5 min. Cloning was done using the NEBuilder® HiFi DNA Assembly Cloning Kit. For each reaction, the four pieces of DNA were mixed in a 20-µl reaction with the NEBbuilder assembly mix with a final concentration of 0.011 pmol (~ 100 ng) of p201N:Cas9 plasmid, 0.2 pmol of MtU6 amplicon (~ 50 ng), scaffold amplicon (~ 12 ng) and ssDNA gRNA oligo (60-mer, 1 µl). The reactions were incubated at 50 °C for 1 h.

Two µl of the cloning reaction were transformed into 50 µl of One Shot™ Top10 chemically competent cells (Invitrogen, www.thermofisher.com) and plated on lysogeny broth (LB) agar medium (Bertani 1951) with 50 µl/ml kanamycin for transformant selection. Colonies with the correct inserts were screened using the Ubi3p218R and IScelR primers and confirmed by Sanger sequencing (Table S4). Plasmids carrying the designed gRNA constructs were transformed into *Agrobacterium tumefaciens* strain GV3101 for generating transgenic plants.

To avoid off-target effects, gRNAs were further checked by comparison against the reference *N. benthamiana* genome v1.0.1 (www.solgenomics.net). Only two sites were found to have non-target matches > 17 nt (both with 1 internal mismatch), and with the NGG PAM sequence on the correct strand. These two sites were checked by PCR amplification and Sanger sequencing (primers in Table S4) and showed no unexpected editing in our *ASAT* mutant plants.

Stable mutagenesis of ASATs using tissue culture

Stable *ASAT* mutant *N. benthamiana* plants were created in the Boyce Thompson Institute plant transformation facility using CRISPR/Cas9 with gRNAs that had been confirmed to be functional in transient assays (Fig. S9) following a previously described protocol (Van Eck et al. 2019), with minor modifications.

Confirmation of homozygous mutant plants in the T2 generation

Rooted *N. benthamiana* plants from tissue culture were transferred to soil (T0 generation). CRISPR/Cas9-induced mutations were identified by PCR amplification of genomic regions of the gRNA target sites in *ASAT1* and *ASAT2* (Fig. 3), followed by Sanger sequencing (primers in Table S4). Lines with mutations were used to generate T1 plants, which were subjected to PCR amplification and sequencing to confirm homozygous mutations. T2 seeds from confirmed homozygous mutant *asat1-1*, *asat1-2*, *asat2-1*, and *asat2-2* T1 plants were used for all experiments. Homozygous mutations were confirmed in randomly selected T2 plants by PCR amplification and Sanger sequencing. The presence or absence of Cas9 in transgenic plants in the T0, T1, and T2 generations was confirmed by PCR amplification (primers in Table S4) and agarose gel electrophoresis.

Acylsugar measurements by LC/MS

Liquid chromatography/mass spectrometry (LC/MS) was used to measure acylsugar content in leaf extracts from wildtype and *ASAT* mutant plants. New leaflets were rinsed in acylsugar extraction solution (3:3:2 acetonitrile:isopropanol:water, 0.1% formic acid, and 1 µM Telmisartan as internal standard) and gently agitated for 2 min. Then, the extraction solutions were transferred to LC/MS glass vials, and the leaves were air dried for leaf weight measurements.

Chromatography of leaf surface washes was performed using a glass vial autosampler on a ThermoScientific Ultimate 3000 HPLC coupled to a Thermo Scientific Q Exactive™ Hybrid Quadrupole-Orbitrap™ Mass Spectrometer. Acylsugar extracts were separated on an Ascentis Express C18 HPLC column (10 cm × 2.1 mm × 2.7 µm) (Sigma-Aldrich, St. Louis, MO) with a flow rate of 0.3 ml/min, using a gradient flow of 0.1 % formic acid (Solvent A) and 100% acetonitrile (Solvent B). We used a 7-min LC method for metabolite profiling, which involved a linear gradient from 95:5 A:B to 0:98 A:B. Full-scan mass spectra were collected (mass range: m/z 50–1000) in both positive and negative electron spray ionization (ESI) modes. Mass spectral parameters were set as follows: capillary spray voltage 2.00 kV for negative ion-mode and 3.00 kV for positive ion-mode, source temperature: 100 °C, desolvation temperature 350 °C, desolvation nitrogen gas flow rate: 600 L/h, cone voltage 35 V. Acylsugars were identified and annotated using Thermo Xcalibur Qual Browser (Thermo Fisher) and MS-DIAL v4.20 based on the MS/MS peak features and neutral losses (Fig. S3). The acylsugar abundances were estimated using peak areas at the respective *m/z* channel under negative ESI mode. Acylsugar quantification was first normalized to the internal control Telmisartan to account for technical variation, and then normalized to the leaf dry weight to allow comparisons between samples.

Insect choice and no-choice bioassays

To measure *M. persicae* and *M. euphorbiae* growth, we caged aphids on individual leaves of mutant and wildtype 4 to 5-week-old *N. benthamiana* (Fig. S10a, b). Twenty adult *M. persicae* from *N. tabacum* (naïve to *N. benthamiana*) were placed in each cage and allowed to generate nymphs for ~ 12 h. Twenty-five nymphs were left in each cage and were monitored for 5 days to assess nymph survival. At the end of the survival monitoring period, five *M. persicae* were left in each cage and reproduction was monitored for one week. The remaining *M. persicae* were collected to measure aphid size by imaging and assessing the area of each aphid using ImageJ (Schneider et al. 2012). Ten adult *M. euphorbiae* from a colony on tomato cv. Moneymaker were placed in each individual cage on *N. benthamiana* leaves. Surviving aphids and progeny were counted after 24 h.

M. persicae and *M. euphorbiae* choice assays were performed with detached leaves from 4 to 5-week-old *N. benthamiana*. Two similarly sized leaves from individual *ASAT* mutant and wildtype plants were cut and placed in 15-cm Petri dishes, with their petioles inserted in moistened cotton swabs (Fig. S10c). Ten adult aphids were released at the midpoint between pairs of leaves (wildtype, *asat1*, or *asat2*), and the Petri dishes were placed under 16:8 h light:dark photoperiod. The aphids on each leaf were counted at 24 h after their release in the Petri dishes.

To measure whitefly survival and fecundity on wildtype and *asat2-1 N. benthamiana* plants, cages were set up with plants at the seven-leaf stage (~ 3 weeks old). Each cage contained three plants, either wildtype or *asat2-1*. Ninety adult whiteflies reared on *Brassica oleracea* (variety Earliana; www.burpee.com, catalog# 62729 A) were introduced into each cage (60 × 60 × 60 cm) with *N. benthamiana* (30 whiteflies/plant) and were allowed to feed for three days at 26 °C with a 16:8 h light:dark photoperiod. The numbers of whiteflies surviving on each host plant were counted, after which the remaining insects were killed with insecticidal soap. The following day, the number of whitefly eggs on each plant was counted. This experiment was conducted twice with similar results.

For whitefly choice assays, wildtype and *asat2-1* plants at the seven-leaf stage were placed together in the same cage. Approximately 150 whiteflies from cabbage plants were moved into each cage. After 24 h at 26 °C with a 16:8 h light:dark photoperiod, live and dead whiteflies were counted on the plants and elsewhere in the cage. This experiment was repeated three times.

Eggs of *H. zea, H. virescens*, and *T. ni* were hatched on artificial diet (beet armyworm diet, Southland Products, Lake Village, Arkansas). Neonate larvae were confined onto individual *N. benthamiana* leaves, one larva/plant, using 10 × 15 cm organza mesh bags (www.amazon.com, item B073J4RS9C). After ten days, the surviving larvae were counted and weighed. In a separate experiment, *H. zea, H. virescens*, and *T. ni* were reared on artificial diet for five days. Individual five-day-old caterpillars were weighed and then confined on 4 to 4.5-week-old *N benthamiana* plants using 30 cm x 60 cm micro-perforated bread bags (www.amazon.com). After seven days, the surviving larvae were weighed again. Relative growth rate was calculated as: ln(((day-12 mass)/(mean day-5 mass))/7).

Leaf water loss and temperature assays

To measure the leaf water loss, two leaves from each of eight plants were detached. The fresh weight of each leaf was determined on a Sartorius Ultra Micro Balance. All leaves were placed at 23 °C and a 16:8 h light:dark photoperiod. Each leaf was weighted again after 24 h and the percent water loss was calculated as [(fresh_weight – final_weight)/fresh_weight] × 100 %.

Thermal images were acquired in a growth chamber using a thermal camera (A655sc, FLIR Systems Inc., Boston, MA) with a spectral range of 7.5–14.0 mm and a resolution of 640 × 480 pixels. The camera was placed ~ 1 m away from each plant in front of a white background. One region of interest, corresponding to the perimeter of each leaf, was specified per leaf for 20 leaves per genotype. Using the FLIR ResearchIR Max software v.4.40.9.30, thermal images files were exported as CSV files. Images were segmented from the background using Gaussian mixture models in MATLAB to determine the temperature of each leaf. After segmentation, the temperature was averaged across the segmented leaf.

Hyperspectral images were acquired in a dark room using a hyperspectral imager (SOC710, Series 70-V, Surface Optics Corporation, San Diego, CA) that covered a 400–1000 nm spectral range for 128 wavebands. Image acquisition was performed using a Dell DELL XPS 15 9570 laptop computer that controlled the camera. The camera was fixed ~ 1 m above the plants and captured top view images. A Spectralon tile (Labsphere Inc, North Sutton, NH) was placed next to the plant trays, covering one corner of the image to facilitate subsequent image processing and calibration. The nominal reflectance value for the Spectralon tile was 99% with a 30.5 × 30.5 cm^2 reflective area. Lighting consisted of two halogen lamps placed at ~ 45° angles on either side of the camera to create an even light distribution. All image analysis was performed in HSIviewer, a MATLAB package (Stone et al. 2020). White reflectance calibration was performed using the Spectralon tile. One region of interest was specified for each of 20 leaves per genotype. This region of interest corresponded to the perimeter of each leaf. From each hyperspectral cube image, the vegetation pixels (green portion of the plant) were extracted using the Normalized Difference Vegetation Index (NDVI). Mean reflectance (R) was calculated per band per 10 leaves in order to obtain the water band index (WBI) results. To calculate NDVI and WBI we used the following formulas, where *R* corresponds to the reflectance at a specific wavelength (nm): WBI = (R970/R900) (Penuelas et al. 1993) and NVDI = (R750 − R705)/(R750 + R705) (Gitelson and Merzlyak 1994).

Statistical analysis

All statistical comparisons were conducted using SPSS v25, R and MATLAB R2019a (MathWorks, Inc., Natick, MA, USA). ANOVA followed by a Dunnett's post hoc test was used to determine differences in leaf water loss, leaf temperature, and WBI across genotypes in each data set. ANOVA followed by a Duncan post hoc test was used for aphid bioassay and LC/MS results. A Chi-squared test was used to test for differences in pairwise aphid choice assays, whitefly, and lepidopteran assays. Raw data for all figures are shown in Table S3.

Supplementary Information The online version contains supplementary material available at https://doi.org/10.1007/s11103-021-01191-3.

Acknowledgements We thank Patricia Keen and Joyce Van Eck for their help with *N. benthamiana* stable transformation, Ning Zhang and Greg Martin for sharing the p201N-Cas9 construct and the *Drm3* sgRNA control constructs, and William Stone and Thomas Lawton for providing custom image processing software.

Author contributions GJ and HF conceived the original research plans; HF, SS, LA, HX, LK, JDT, SHC, and ANF performed the experiments; HF, LA, LK, and GDM analyzed the data; CLC, MAG, GDM, GS, and GJ supervised the experiments; HF and GJ wrote the article with contributions from all of the authors; GJ agrees to serve as the contact author responsible for communication and distribution of samples.

Funding This research was supported by Cornell startup funds to G.D.M., Deutsche Forschungsgemeinschaft award #411255989 to L.H.K., and United States Department of Agriculture Biotechnology Risk Assessment Grant 2017-33522-27006, US National Science Foundation award IOS-1645256, and Defense Advanced Research Projects Agency (DARPA) agreement HR0011-17-2-0053 to G.J, and US National Science Foundation award #1723926 to C.L.C. G.S. is part of a team supporting DARPA's Insect Allies program under agreement HR0011-17-2-0055. M.A.G. is part of a team supporting DARPA's Advanced Plant Technologies program under agreement HR0011-18-C-0146. The views and conclusions contained in this document are those of the authors and should not be interpreted as representing the official policies of the U.S. Government.

Data availability All data generated or analyzed during this study are included in this published article and its supplementary information files.

Declarations

Conflict of interest The authors declare that there is no conflict of interest.

References

Arntzen C (2015) Plant-made pharmaceuticals: from 'Edible Vaccines' to Ebola therapeutics. Plant Biotechnol J 13:1013–1016

Arrendale RF, Severson RF, Sisson VA, Costello CE, Leary JA, Himmelsbach DS, Vanhalbeek H (1990) Characterization of the sucrose ester fraction from *Nicotiana glutinosa*. J Agric Food Chem 38:75–85

Bally J, Jung H, Mortimer C, Naim F, Philips JG, Hellens R, Bombarely A, Goodin MM, Waterhouse PM (2018) The rise and rise of *Nicotiana benthamiana*: a plant for all reasons. Ann Rev Phytopathol 56 56:405–426

Bertani G (1951) Studies on lysogenesis. I. The mode of phage liberation by lysogenic *Escherichia coli*. J Bacteriol 62:293–300

Bombarely A, Rosli HG, Vrebalov J, Moffett P, Mueller LA, Martin GB (2012) A draft genome sequence of *Nicotiana benthamiana* to enhance molecular plant-microbe biology research. Mol Plant-Micr Int 25:1523–1530

Bos JI, Prince D, Pitino M, Maffei ME, Win J, Hogenhout SA (2010) A functional genomics approach identifies candidate effectors from the aphid species Myzus persicae (green peach aphid). PLoS Genet 6:e1001216

Capella-Gutierrez S, Silla-Martinez JM, Gabaldon T (2009) trimAl: a tool for automated alignment trimming in large-scale phylogenetic analyses. Bioinformatics 25:1972–1973

Cardoso MZ (2008) Herbivore handling of a plant's trichome: The case of *Heliconius charithonia* (L.) (Lepidoptera: Nymphalidae) and *Passiflora Lobata* (Killip) Hutch. (Passifloraceae). Neotropical Entomol 37:247–252

Casteel CL, Yang C, Nanduri AC, **De** Jong HN, Whitham SA, Jander G (2014) The NIa-Pro protein of turnip mosaic virus improves growth and reproduction of the aphid vector, *Myzus persicae* (green peach aphid). Plant J 77: 653–663

Chortyk OT, Pomonis JG, Johnson AW (1996) Syntheses and characterizations of insecticidal sucrose esters. J Ag Food Chem 44:1551–1557

Chortyk OT, Severson RF, Cutler HC, Sisson VA (1993) Antibiotic activities of sugar esters isolated from selected *Nicotiana* species. Biosci Biotechnol Biochem 57:1355–1356

Clay N, Adio A, Denoux C, Jander G, Ausubel F (2009) Glucosinolate metabolites required for an Arabidopsis innate immune response. Science 323:95–101

D'Auria JC (2006) Acyltransferases in plants: a good time to be BAHD. Curr Opin Plant Biol 9: 331–340

Egan AN, Moore S, Stellari GM, Kang BC, Jahn MM (2019) Tandem gene duplication and recombination at the AT3 locus in the *Solanaceae*, a gene essential for capsaicinoid biosynthesis in *Capsicum*. Plos One 14:e0210510

Egea I, Albaladejo I, Meco V, Morales B, Sevilla A, Bolarin MC, Flores FB (2018) The drought-tolerant *Solanum pennellii* regulates leaf water loss and induces genes involved in amino acid and ethylene/jasmonate metabolism under dehydration. Sci Rep 8:2791

Ellison EE, Nagalakshmi U, Gamo ME, Huang PJ, Dinesh-Kumar S, Voytas DF (2020) Multiplexed heritable gene editing using RNA viruses and mobile single guide RNAs. Nat Plants 6:620–624

Elzinga DA, **De** Vos M, Jander G (2014) Suppression of plant defenses by a *Myzus persicae* (green peach aphid) salivary effector protein. Mol Plant Microbe Interact 27: 747–756

Fan P, Leong BJ, Last RL (2019) Tip of the trichome: evolution of acylsugar metabolic diversity in Solanaceae. Curr Opin Plant Biol 49:8–16

Fan P, Miller AM, Schilmiller AL, Liu X, Ofner I, Jones AD, Zamir D, Last RL (2016) In vitro reconstruction and analysis of evolutionary variation of the tomato acylsucrose metabolic network. Proc Natl Acad Sci USA 113:E239–E248

Feng H, Jander G (2021) Rapid screening of emopenMyzus persicaeemclose (green peach aphid) RNAi targets using emopenTobacco rattle virusemclose. Methods Mol Biol 2360:105–117

Fobes JF, Mudd JB, Marsden MP (1985) Epicuticular lipid accumulation on the leaves of *Lycopersicon pennellii* (Corr.) D'Arcy and *Lycopersicon esculentum* Mill. Plant Physiol 77:567–570

Gaquerel E, Kotkar H, Onkokesung N, Galis I, Baldwin IT (2013) Silencing an N-acyltransferase-like involved in lignin biosynthesis in *Nicotiana attenuata* dramatically alters herbivory-induced phenolamide metabolism. Plos One 8:e62336

Gitelson A, Merzlyak MN (1994) Spectral reflectance changes associated with autumn senescence of *Aesculus hippocastanum* L. and *Acer platanoides* L. leaves - spectral features and relation to chlorophyll estimation. J Plant Physiol 143:286–292

Glas JJ, Schimmel BCJ, Alba JM, Escobar-Bravo R, Schuurink RC, Kant MR (2012) Plant glandular trichomes as targets for breeding or engineering of resistance to herbivores. Int J Mol Sci 13:17077–17103

Gong P, Zhang J, Li H, Yang C, Zhang C, Zhang X, Khurram Z, Zhang Y, Wang T, Fei Z, Ye Z (2010) Transcriptional profiles of drought-responsive genes in modulating transcription signal transduction, and biochemical pathways in tomato. J Exp Bot 61:3563–3575

Goodin MM, Zaitlin D, Naidu RA, Lommel SA (2008) *Nicotiana benthamiana*: its history and future as a model for plant-pathogen interactions. Mol Plant Microbe Interact 21:1015–1026

Hagimori M, Matsui M, Matsuzaki T, Shinozaki Y, Shinoda T, Harada H (1993) Production of somatic hybrids between *Nicotiana benthamiana* and *Nicotiana tabacum* and their resistance to aphids. Plant Sci 91:213–222

Jacobs TB, LaFayette PR, Schmitz RJ, Parrott WA (2015) Targeted genome modifications in soybean with CRISPR/Cas9. Bmc Biotechnol 15:16

Karabourniotis G, Kotsabassidis D, Manetas Y (1995) Trichome density and its protective potential against ultraviolet-B radiation damage during leaf development. Canadian J Botany Revue Canadienne De Botanique 73:376–383

Kim J, Kang K, Gonzales-Vigil E, Shi F, Jones AD, Barry CS, Last RL (2012) Striking natural diversity in glandular trichome acylsugar composition is shaped by variation at the Acyltransferase2 locus in the wild tomato Solanum habrochaites. Plant Physiol 160:1854–1870

Kroumova AB, Wagner GJ (2003) Different elongation pathways in the biosynthesis of acyl groups of trichome exudate sugar esters from various solanaceous plants. Planta 216:1013–1021

Kroumova ABM, Zaitlin D, Wagner GJ (2016) Natural variability in acyl moieties of sugar esters produced by certain tobacco and other *Solanaceae* species. Phytochemistry 130:218–227

Landis JB, Miller CM, Broz AK, Bennett AA, Carrasquilla-Garcia N, Cook DR, Last RL, Bedinger PA, Moghe GD (2021) Migration through a major Andean ecogeographic disruption as a driver of genetic and phenotypic diversity in a wild tomato species. Mol Biol Evol 38:3202–3219

Laue G, Preston CA, Baldwin IT (2000) Fast track to the trichome: induction of N-acyl nornicotines precedes nicotine induction in *Nicotiana repanda*. Planta 210:510–514

Leong BJ, Hurney SM, Fiesel PD, Moghe GD, Jones AD, Last RL (2020) Specialized metabolism in a nonmodel nightshade: Trichome acylinositol biosynthesis. Plant Physiol 183:915–924

Leong BJ, Lybrand DB, Lou YR, Fan PX, Schilmiller AL, Last RL (2019) Evolution of metabolic novelty: A trichome-expressed invertase creates specialized metabolic diversity in wild tomato. Sci Adv 5:eaaw3754

Liu H, Ding YD, Zhou YQ, Jin WQ, Xie KB, Chen LL (2017) CRISPR-P 2.0: an improved CRISPR-Cas9 tool for genome editing in plants. Mol Plant 10:530–532

Lou YR, Anthony TM, Fiesel PD, Arking RE, Christensen EM, Jones AD, Last RL (2021) It happened again: convergent evolution of acylglucose specialized metabolism in black nightshade and wild tomato. 10.1101/2021.06.08.447545

Luu VT, Weinhold A, Ullah C, Dressel S, Schoettner M, Gase K, Gaquerel E, Xu S, Baldwin IT (2017) *O*-Acyl sugars protect a wild tobacco from both native fungal pathogens and a specialist herbivore. Plant Physiol 174:370–386

Marchant WG, Legarrea S, Smeda JR, Mutschler MA, Srinivasan R (2020) Evaluating acylsugars-mediated resistance in tomato against *Bemisia tabaci* and transmission of tomato yyellow leaf curl virus. Insects 11:842

Matsuzaki T, Shinozaki Y, Hagimori M, Tobita T, Shigematsu H, Koiwai A (1992) Novel glycerolipids and glycolipids from the surface-lipids of *Nicotiana benthamiana*. Biosci Biotechnol Biochem 56:1565–1569

Matsuzaki T, Shinozaki Y, Suhara S, Ninomiya M, Shigematsu H, Koiwai A (1989) Isolation of glycolipids from the surface-lipids of *Nicotiana bigelovii* and their distribution in *Nicotiana* species. Agric Biol Chem 53:3079–3082

McKenzie CL, Puterka GJ (2004) Effect of sucrose octanoate on survival of nymphal and adult *Diaphorina citri* (Homoptera: Psyllidae). J Econ Entomol 97:970–975

McKenzie CL, Weathersbee AA, **3rd**, Puterka GJ (2005) Toxicity of sucrose octanoate to egg, nymphal, and adult *Bemisia tabaci* (Hemiptera: Aleyrodidae) using a novel plant-based bioassay. J Econ Entomol 98: 1242–1247

Meihls LN, Handrick V, Glauser G, Barbier H, Kaur H, Haribal MM, Lipka AE, Gershenzon J, Buckler ES, Erb M, Köllner TG, Jander G (2013) Natural variation in maize aphid resistance is associated with 2,4-dihydroxy-7-methoxy-1,4-benzoxazin-3-one glucoside methyltransferase activity. Plant Cell 25:2341–2355

Moghe GD, Leong BJ, Hurney SM, Daniel Jones A, Last RL (2017) Evolutionary routes to biochemical innovation revealed by integrative analysis of a plant-defense related specialized metabolic pathway. Elife 6:e28468

Nadakuduti SS, Uebler JB, Liu X, Jones AD, Barry CS (2017) Characterization of trichome-expressed BAHD acyltransferases in *Petunia axillaris* reveals distinct acylsugar assembly mechanisms within the Solanaceae. Plant Physiol 175:36–50

Ning J, Moghe GD, Leong B, Kim J, Ofner I, Wang Z, Adams C, Jones AD, Zamir D, Last RL (2015) A feedback-insensitive isopropylmalate synthase affects acylsugar composition in cultivated and wild tomato. Plant Physiol 169:1821–1835

Nonomura T, Xu L, Wada M, Kawamura S, Miyajima T, Nishitomi A, Kakutani K, Takikawa Y, Matsuda Y, Toyoda H (2009) Trichome exudates of *Lycopersicon pennellii* form a chemical barrier to suppress leaf-surface germination of *Oidium neolycopersici* conidia. Plant Sci 176:31–37

O'Connell MA, Medina AL, Sanchez Pena P, Trevino MB (2007) Molecular genetics of drought resistance response in tomato and related species. In: Razdan MK, Mattoo AK (eds). Genetic improvement of solanaceous crops Enfield USA, pp 261–283

Penuelas J, Filella I, Biel C, Serrano L, Save R (1993) The reflectance at the 950–970 nm region as an indicator of plant water status. Int J Remote Sens 14:1887–1905

Powell JD (2015) From pandemic preparedness to biofuel production: tobacco finds its biotechnology niche in North America. Agriculture Basel 5:901–917

Ramsey JS, Elzinga DA, Sarkar P, Xin YR, Ghanim M, Jander G (2014) Adaptation to nicotine feeding in *Myzus persicae*. J Chem Ecol 40:869–877

Ramsey JS, Wilson AC, **De** Vos M, Sun Q, Tamborindeguy C, Winfield A, Malloch G, Smith DM, Fenton B, Gray SM, Jander G (2007) Genomic resources for *Myzus persicae*: EST sequencing, SNP identification, and microarray design. BMC Genom 8: 423

Rodriguez AE, Tingey WM, Mutschler MA (1993) Acylsugars of *Lycopersicon pennellii* deter settling and feeding of the green peach aphid (Homoptera, Aphididae). J Econ Entomol 86:34–39

Rodriguez PA, Stam R, Warbroek T, Bos JI (2014) Mp10 and Mp42 from the aphid species Myzus persicae trigger plant defenses in Nicotiana benthamiana through different activities. Mol Plant Microbe Interact 27:30–39

Schiavinato M, Strasser R, Mach L, Dohm JC, Himmelbauer H (2019) Genome and transcriptome characterization of the glycoengineered *Nicotiana benthamiana* line DeltaXT/FT. BMC Genom 20:594

Schilmiller A, Shi F, Kim J, Charbonneau AL, Holmes D, Jones AD, Last RL (2010) Mass spectrometry screening reveals widespread diversity in trichome specialized metabolites of tomato chromosomal substitution lines. Plant J 62:391–403

Schilmiller AL, Charbonneau AL, Last RL (2012) Identification of a BAHD acetyltransferase that produces protective acyl sugars in tomato trichomes. Proc Natl Acad Sci USA 109:16377–16382

Schilmiller AL, Moghe GD, Fan P, Ghosh B, Ning J, Jones AD, Last RL (2015) Functionally divergent alleles and duplicated loci encoding an acyltransferase contribute to acylsugar metabolite diversity in *Solanum* trichomes. Plant Cell 27:1002–1017

Schneider CA, Rasband WS, Eliceiri KW (2012) NIH Image to ImageJ: 25 years of image analysis. Nat Methods 9:671–675

Shepherd RW, Wagner GJ (2007) Phylloplane proteins: emerging defenses at the aerial frontline? Trends Plant Sci 12:51–56

Simmons AT, Gurr GM, McGrath D, Martin PM, Nicol HI (2004) Entrapment of *Helicoverpa armigera* (Hubner) (Lepidoptera:Noctuidae) on glandular trichomes of *Lycopersicon* species. Aust J Entomol 43:196–200

Simon B, Cenis JL, Demichelis S, Rapisarda C, Caciagli P, Bosco D (2003) Survey of *Bemisia tabaci* (Hemiptera: Aleyrodidae) biotypes in Italy with the description of a new biotype (T) from *Euphorbia characias*. Bull Entomol Res 93:259–264

Slocombe SP, Schauvinhold I, McQuinn RP, Besser K, Welsby NA, Harper A, Aziz N, Li Y, Larson TR, Giovannoni J, Dixon RA, Broun P (2008) Transcriptomic and reverse genetic analyses of branched-chain fatty acid and acyl sugar production in *Solanum pennellii* and *Nicotiana benthamiana*. Plant Physiol 148:1830–1846

Song Z, Li S, Chen X, Liu L, Song Z (2006) Synthesis of sucrose esters. For Stud China 8:26–29

Stamatakis A (2014) RAxML version 8: a tool for phylogenetic analysis and post-analysis of large phylogenies. Bioinformatics 30:1312–1313

Stone WD, Pellicore MJ, Hagstrom S, Lawton TJ (2020) HSIviewer: pushbutton hyperspectral image analysis for rapid plant phenotyping. in review

Thompson JD, Higgins DG, Gibson TJ (1994) Clustal-W - Improving the sensitivity of progressive multiple sequence alignment through sequence weighting, position-specific gap penalties and weight matrix choice. Nucleic Acids Res 22:4673–4680

Thurston R (1961) Resistance in *Nicotiana* to the green peach aphids and some other tobacco insect pest. J Econ Entomol 54:946–949

Van Eck J, Keen P, Tjahjadi M (2019) *Agrobacterium tumefaciens*-mediated transformation of tomato. Methods Mol Biol 1864: 225–234

Van T, Weinhold A, Ullah C, Dressel S, Schoettner M, Gase K, Gaquerel E, Xu SQ, Baldwin IT (2017) O-acyl sugars protect a wild tobacco from both native fungal pathogens and a specialist herbivore. Plant Physiol 174:370–386

Wagner GJ, Wang E, Shepherd RW (2004) New approaches for studying and exploiting an old protuberance, the plant trichome. Ann Bot 93:3–11

Weinhold A, Baldwin IT (2011) Trichome-derived O-acyl sugars are a first meal for caterpillars that tags them for predation. Proc Natl Acad Sci USA 108:7855–7859